# Improved transverse $(e, e')$ response function of $^3$He at intermediate momentum transfers

Victor D. Efros,[1] Winfried Leidemann,[2,*] Giuseppina Orlandini,[2] and Edward L. Tomusiak[3]

[1]*Russian Research Centre Kurchatov Institute, RU-123182 Moscow, Russia*

[2]*Dipartimento di Fisica, Università di Trento, and Istituto Nazionale di Fisica Nucleare, Gruppo Collegato di Trento, I-38050 Povo, Italy*

[3]*Department of Physics and Astronomy, University of Victoria, Victoria, V8P 1A1 British Columbia, Canada*

(Received 13 October 2009; published 4 March 2010)

The transverse electron scattering response function of $^3$He is studied in the quasielastic peak region for momentum transfers between 500 and 700 MeV/$c$. A conventional description of the process leads to results that vary substantially from experiment. To improve the results, the present calculation is done in a reference frame [the active nucleon Breit (ANB) frame] that diminishes the influence of relativistic effects on nuclear states. The laboratory frame response function is then obtained via a kinematics transformation. In addition, a one-body nuclear current operator is employed that includes all leading-order relativistic corrections. Multipoles of this operator are listed. It is shown that the use of the ANB frame leads to a sizable shift in the quasielastic peak to lower energy and, contrary to the relativistic current, also to an increase in the peak height. The additionally considered meson exchange current contribution is quite small in the peak region. In comparison with experiment, there is excellent agreement of the peak positions. The peak height agrees well with experiment for the lowest considered momentum transfer (500 MeV/$c$) but tends to be too high for higher momentum transfer (10% at 700 MeV/$c$).

DOI: 10.1103/PhysRevC.81.034001 PACS number(s): 25.30.Fj, 21.45.−v, 21.30.−x

## I. INTRODUCTION

In Ref. [1] we studied the longitudinal electron scattering response function of trinucleons. We, as well as others [1–3], observed that for increasing momentum transfer $q$, in particular, for $q > 500$ MeV/$c$, the nonrelativistic theoretical results increasingly deviate from experiment. A similar problem arises in the case of the transverse response of trinucleons [2–4]. These problems appear to be related in part to a deficiency of the nonrelativistic nuclear dynamics at such $q$ values. In Ref. [5] methods were proposed that would allow the extension of such nonrelativistic calculations to higher $q$. These methods proved to be efficient in the case of the longitudinal response.

In the present work, with the help of one of these methods we analyze the transverse response function of $^3$He in the quasielastic peak region. Another improvement on the nonrelativistic description in the present work results from our taking into account all the leading-order relativistic corrections to the one-body electromagnetic current operator. Such corrections have been employed in the deuteron case [6] and they were included [2,3] when calculating magnetic form factors for elastic electron scattering on trinucleons. However, they have not been previously taken into account for the $A = 3$ transverse responses. Here we account for these corrections via consideration of the current operator that contains all the correction terms of the $M^{-3}$ order. We calculate this operator proceeding from corresponding matrix elements [6] of the current.

Our preceding study of the transverse response of $^3$He [4] was done in the framework of a nonrelativistic description with inclusion of the full final-state interaction via the Lorentz integral transform method [7,8]. We used the BonnA *NN* potential [9] plus conventional *NNN* forces as a nuclear dynamics input. Use of the BonnA potential gave a "unique" prescription for meson exchange contributions to the electromagnetic current of the nucleus. It is of interest, however, to use for the present study more modern *NN* interactions such as the AV18 potential [10]. Our results for the transverse response functions of trinucleons using the AV18 *NN* plus UIX *NNN* [11] potentials recently appeared [12] for the threshold region. In that paper we describe our procedure for using the Arenhövel-Schwamb technique [13] meson exchange currents (MECs) of the AV18 potential. In the present work we extend our considerations to the quasielastic region and consider various intermediate momentum transfers.

## II. FORMULATION

In the one-photon exchange approximation the cross section for the process of inclusive electron scattering on a nucleus is given by

$$\frac{d^2\sigma}{d\Omega d\omega} = \sigma_{\rm Mott}\left[\frac{Q^4}{q_{\rm lab}^4}R_L(q_{\rm lab},\omega_{\rm lab}) + \left(\frac{Q^2}{2q_{\rm lab}^2}+\tan^2\frac{\theta}{2}\right)R_T(q_{\rm lab},\omega_{\rm lab})\right], \quad (1)$$

where $R_L$ and $R_T$ are the longitudinal and transverse response functions, respectively, $\omega_{\rm lab}$ is the electron energy loss, $q_{\rm lab}$ is the magnitude of the electron momentum transfer, $\theta$ is the electron scattering angle, and $Q^2 = q_{\rm lab}^2 - \omega_{\rm lab}^2$.

In the present work we study the transverse response function. It may be written as

$$R_T(q_{\rm lab},\omega_{\rm lab}) = \overline{\sum}_{M_i}\iint df\,(\mathbf{J}_t^\dagger)_{i\bar f}\cdot(\mathbf{J}_t)_{\bar f i}\,\delta(E_{\bar f}-E_i-\omega_{\rm lab}). \quad (2)$$

*leideman@science.unitn.it

 

Here the subscripts $i$ and $\bar{f}$ label, respectively, the initial state and final states including their total momenta $\mathbf{P}_i$ and $\mathbf{P}_{\bar{f}}$. The set $\bar{f}$ includes $\mathbf{P}_{\bar{f}}$ and additional asymptotic quantum numbers, which we denote $f$. One may write $d\bar{f} = d\mathbf{P}_{\bar{f}} df$. Equation (2) contains $df$ only. The notation $E_i$ and $E_{\bar{f}}$ refers to total initial- and final-state energies. (In Ref. [4] the notation $E_{i,f}$ was used for internal energies.) The quantities $(\mathbf{J}_t)_{\bar{f}i}$ are on-shell matrix elements of the transverse component of the nuclear current operator $\bar{\mathbf{J}}(\mathbf{q}, \omega)$,

$$(\mathbf{J}_t)_{\bar{f}i}\delta(\mathbf{P}_{\bar{f}} - \mathbf{P}_i - \mathbf{q}) = \langle \Psi_{\bar{f}}|\bar{\mathbf{J}}_t(\mathbf{q}, \omega)|\Psi_i\rangle, \tag{3}$$

taken at $\mathbf{q} = \mathbf{q}_{\rm lab}$, $\omega = \omega_{\rm lab}$, and $\mathbf{P}_i = 0$. The states entering here are eigenstates of the total Hamiltonian with eigenenergies $E_{\bar{f}}$ and $E_i$. They are normalized as

$$\begin{aligned}\langle \Psi_{\bar{f}}|\Psi_{\bar{f}'}\rangle &= \delta(\bar{f} - \bar{f}') = \delta(\mathbf{P}_{\bar{f}} - \mathbf{P}_{\bar{f}'})\delta(f - f'),\\ \langle \Psi_i|\Psi_{i'}\rangle &= \delta(\mathbf{P}_i - \mathbf{P}_{i'}).\end{aligned} \tag{4}$$

These relationships refer to the laboratory reference frame. It is also useful to consider a response-type quantity $R_T^{\rm fr}$ defined by the same relationships referring to another reference frame. We denote the corresponding quantities $q_{\rm fr}$, etc. In particular, the states $\Psi_{\bar{f}}$ and $\Psi_i$ then will be eigenstates of the total Hamiltonian in the reference frame considered. For the class of reference frames moving with respect to the laboratory frame along the $\mathbf{q}$ direction, the following relationship is valid:

$$R_T(q_{\rm lab}, \omega_{\rm lab}) = \frac{E_i^{\rm fr}}{M_T} R_T^{\rm fr}(q_{\rm fr}, \omega_{\rm fr}). \tag{5}$$

Here $M_T$ is the mass of the target.

Relativistic effects are present in Eq. (3) both in the states $\Psi_i$ and $\Psi_{\bar{f}}$ and in the nuclear current operator. To account for the former effects we proceed as in the longitudinal case [5] and introduce the active nucleon Breit (ANB) frame. In the ANB frame, the nucleus has the momentum $-A\mathbf{q}_{\rm ANB}/2$ in the initial state, $\mathbf{q}_{\rm ANB}$ being the momentum transfer from the electron to the nucleus in this reference frame. At high $q$ values, nucleon momenta in the initial state have the values of about $-\mathbf{q}_{\rm ANB}/2$ in this reference frame. In the final state in quasifree kinematics the active nucleon has a momentum of about $\mathbf{q}_{\rm ANB}/2$, while the momentum of each of the other nucleons remains at about $-\mathbf{q}_{\rm ANB}/2$. Thus, the typical initial- and final-state nucleon momenta are restricted to magnitudes of about $q_{\rm ANB}/2 \simeq q/2$ in the ANB reference frame, while, say, in the laboratory frame nucleon momenta up to $q$ are present. Furthermore, it also follows from the preceding that the energy transfer $\omega_{\rm ANB}$ in the ANB reference frame is zero at the quasielastic peak, and this applies to both the relativistic and the nonrelativistic case. Therefore, even when one treats the nucleus nonrelativistically the peak remains at the same position as in the relativistic case. This contrasts with a description of the process in the laboratory reference frame, where positions of the peak in the relativistic and the nonrelativistic cases would differ considerably. Hence one expects that performing nonrelativistic calculations in the quasielastic region in the ANB frame minimizes errors owing to kinematic relativistic effects. This expectation proves true in the longitudinal case [5]. The laboratory response function sought for is obtained subsequently with the help of Eq. (5), with "ANB" being substituted for "fr."

We perform the corresponding nonrelativistic calculation in the ANB reference frame. One defines the internal current operator $\mathbf{J}$ obtained by taking a matrix element in the center-of-mass subspace of the total current operator:

$$\mathbf{J}\delta(\mathbf{P}_{\bar{f}} - \mathbf{P}_i - \mathbf{q}) = \langle \mathbf{P}_{\bar{f}}|\bar{\mathbf{J}}(\mathbf{q}, \omega)|\mathbf{P}_i\rangle. \tag{6}$$

At $\mathbf{P}_i = P_i\hat{\mathbf{q}}$, $\hat{\mathbf{q}}$ being $q^{-1}\mathbf{q}$, this operator may be written as $\mathbf{J}(\mathbf{q}, \omega, P_i)$. One may then rewrite Eq. (2) as

$$\begin{aligned}R_T^{\rm ANB}(q_{\rm ANB}, \omega_{\rm ANB}) = \overline{\sum}_{M_i} \int\!\!\!\!\!\!\int df\, \langle \psi_i|\mathbf{J}_t^\dagger|\psi_f\rangle\\ \cdot \langle \psi_f|\mathbf{J}_t|\psi_i\rangle \delta[e_f - e(q_{\rm ANB}, \omega_{\rm ANB})],\end{aligned} \tag{7}$$

where the transverse component $\mathbf{J}_t$ of $\mathbf{J}(\mathbf{q}, \omega, P_i)$ is used and the values $\mathbf{q} = \mathbf{q}_{\rm ANB}$, $\omega = \omega_{\rm ANB}$, and $P_i = -Aq_{\rm ANB}/2$ are set. Here $\psi_i$ and $\psi_f$ are the nonrelativistic internal states. They are independent of the center-of-mass momenta. The energy $e_f$ is the internal energy in the final state, and

$$\begin{aligned}e(q_{\rm ANB}, \omega_{\rm ANB}) &= e_i + \omega_{\rm ANB} + \frac{\left(P_i^{\rm ANB}\right)^2 - \left(P_f^{\rm ANB}\right)^2}{2M_T}\\ &= e_i + \omega_{\rm ANB} + \frac{(A-1)q_{\rm ANB}^2}{2M_T},\end{aligned} \tag{8}$$

where $e_i$ is the internal energy in the initial state. One also has

$$\begin{aligned}q_{\rm ANB} &= \gamma(q_{\rm lab} - \beta\omega_{\rm lab}),\\ \omega_{\rm ANB} &= \gamma(\omega_{\rm lab} - \beta q_{\rm lab}), \quad \gamma = (1-\beta^2)^{-1/2},\end{aligned} \tag{9}$$

$$\begin{aligned}\left[M_T^2 + \left(P_i^{\rm ANB}\right)^2\right]^{1/2} &= \gamma M_T,\\ \beta &= \frac{q_{\rm lab}}{2(M_T/A)}\left[1 + \frac{\omega_{\rm lab}}{2(M_T/A)}\right]^{-1}.\end{aligned} \tag{10}$$

(One gets $\omega_{\rm ANB} = 0$ when substituting $\omega_{\rm lab} = [(M_T/A)^2 + q_{\rm lab}^2]^{1/2} - M_T/A$ in the expression for $\omega_{\rm ANB}$. This is in agreement with the preceding statement saying that at the quasielastic peak $\omega_{\rm ANB} = 0$.)

## III. THE NUCLEAR CURRENT OPERATOR AND ITS MULTIPOLE DECOMPOSITION

We employ the transition current operator, which is the sum of one-body and two-body currents. In Ref. [4] the nonrelativistic expression for the one-body current was used. For the present applications we have calculated relativistic corrections to the one-body current operator. To do this we proceeded from the expressions for matrix elements of the one-body current of the form $\langle \mathbf{p}_f|\bar{\mathbf{J}}|\mathbf{p}_i\rangle$ listed in Ref. [6]. The operator so obtained reproduces these expressions.

This operator, denoted $\mathbf{J}^{(1)}$, includes all the relativistic corrections up to order $M^{-2}$, that is, in addition to the nonrelativistic spin current and convection current terms of order $M^{-1}$, it includes all the terms of order $M^{-3}$. Our expression for this operator given here is the internal operator as defined by Eq. (6). We also assume that the initial momentum $\mathbf{P}_i$ is directed along $\mathbf{q}$. (This is the case for the ANB reference

frame.) Then the current operator includes dependence on $\mathbf{q}$, $\omega$, and the magnitude of $\mathbf{P}_i$. In the subsequent expression for it all the momentum operators are placed on the right, hence rendering the operators in nonsymmetric forms. Nevertheless, the hermiticity of $\mathbf{J}(\mathbf{x})$ is still intact but, in momentum space, reads as $\mathbf{J}^\dagger(\mathbf{q}) = \mathbf{J}(-\mathbf{q})$. We use the notation $\mathbf{r}' = \mathbf{r} - \mathbf{R}$ and $\mathbf{p}' = \mathbf{p} - A^{-1}\mathbf{P}$, with $\mathbf{P}$ and $\mathbf{R}$ being the total momentum operator and the nonrelativistic center-of-mass operator.

The resulting one-body current operator is

$$\mathbf{J}^{(1)}(\mathbf{q}, \omega, P_i) = \mathbf{j}_{\rm spin} + \mathbf{j}_p + \mathbf{j}_q + \Delta\mathbf{j} + (\omega/M)\mathbf{j}_\omega, \quad (11)$$

with

$$\mathbf{j}_{\rm spin} = e^{i\mathbf{q}\mathbf{r}'}\frac{i[\vec{\sigma}\times\mathbf{q}]}{2M}\left[G_M\left(1-\frac{q^2}{8M^2}\right) - G_E\frac{\kappa^2 q^2}{8M^2}\right], \quad (12)$$

$$\mathbf{j}_p = e^{i\mathbf{q}\mathbf{r}'}\frac{\mathbf{p}'}{M}\left\{G_E\left[1-\frac{q^2}{8M^2}(\kappa^2+2)\right] + G_M\frac{q^2}{8M^2}\right\}, \quad (13)$$

$$\mathbf{j}_q = e^{i\mathbf{q}\mathbf{r}'}\frac{\kappa\mathbf{q}}{2M}\left\{G_E\left[1-\frac{q^2}{8M^2}(\kappa^2+3)\right] + G_M\frac{q^2}{4M^2}\right\}, \quad (14)$$

$$\begin{aligned}\Delta\mathbf{j} = \frac{e^{i\mathbf{q}\mathbf{r}'}}{8M^3}\{&-2G_E[\kappa\mathbf{q}(p')^2 + 2\mathbf{p}'(p')^2 + 2\kappa\mathbf{p}'(\mathbf{p}'\cdot\mathbf{q})]\\ &+ [G_M - G_E(1+2\kappa^2)]\mathbf{q}(\mathbf{p}'\cdot\mathbf{q})\\ &- 2iG_E[\vec{\sigma}\times\mathbf{q}][(p')^2 + \kappa(\mathbf{p}'\cdot\mathbf{q})]\\ &+ i(G_E - G_M)[\mathbf{p}'\times\mathbf{q}][\kappa(\vec{\sigma}\cdot\mathbf{q}) + 2(\vec{\sigma}\cdot\mathbf{p}')]\},\end{aligned} \quad (15)$$

$$\mathbf{j}_\omega = e^{i\mathbf{q}\mathbf{r}'}\frac{G_E - 2G_M}{8M}(\mathbf{q} + i\kappa[\vec{\sigma}\times\mathbf{q}] + 2i[\vec{\sigma}\times\mathbf{p}']). \quad (16)$$

In the preceding expressions we use the notation

$$G_{E,M} = G^p_{E,M}(Q^2)\frac{1+\tau_z}{2} + G^n_{E,M}(Q^2)\frac{1-\tau_z}{2},$$

where $G^{p,n}_{E,M}$ are the Sachs form factors. We also denote

$$\kappa = 1 + 2P_i/Aq. \quad (17)$$

(Note that $2\mathbf{p} + \mathbf{q} = 2\mathbf{p}' + \kappa\mathbf{q}$.) The terms $\mathbf{j}_p$ and $\mathbf{j}_q$ together represent the convection current. The latter longitudinal component of this current does not enter the net response. However, this component, which contains the charge operator, is required when one uses an alternative expression (the Siegert form; see Eq. (20) in Ref. [4]) for electric multipoles based on the continuity equation. If we chose to use this form in the present calculation, then the charge operator with inclusion of the standard Darwin-Foldy and spin-orbit corrections would be used for calculating electric multipoles. In detail this is given by[1]

$$\rho(\mathbf{q}, \omega) = e^{i\mathbf{q}\mathbf{r}'}\left[G_E\left(1-\frac{q^2}{8M^2}\right) - \frac{G_E - 2G_M}{4M^2}i(\vec{\sigma}\cdot[\mathbf{q}\times\mathbf{p}'])\right]. \quad (18)$$

For the two-body current operator we use the customary nonrelativistic expressions of the form listed in Appendix A in Ref. [4]. The regularization constants entering the two-body current are adjusted to the *NN* interaction we use so that the continuity equation is satisfied approximately; see Ref. [12]. For high $q$ values the relative contribution of the two-body current in the region of the quasielastic peak is less important.

As explained in Ref. [4], the current operator is to be used in the form of an expansion over the multipole operators $T^{\rm el}_{jm}(q, \omega)$ and $T^{\rm mag}_{jm}(q, \omega)$:

$$\mathbf{J}_t = 4\pi\sum_{\lambda={\rm el,mag}}\sum_{jm} i^{j-\epsilon}T^\lambda_{jm}(q, \omega)\mathbf{Y}^{\lambda *}_{jm}(\hat{\mathbf{q}}). \quad (19)$$

Here $\epsilon = 0$ in the electric case and $\epsilon = 1$ in the magnetic case. The quantities $\mathbf{Y}^\lambda_{jm}$ are electric and magnetic vector spherical harmonics [14]. We calculate the multipole operators $T^\lambda_{jm}$ in terms of similar operators $T^l_{jm}$ related to the vector spherical harmonics of the form

$$\mathbf{Y}^l_{jm}(\hat{\mathbf{q}}) = \sum_{m'+\mu=m} C^{jm}_{lm'1\mu}Y_{lm'}(\hat{\mathbf{q}})\mathbf{e}_\mu. \quad (20)$$

Here $\mathbf{e}_\mu$ are the spherical unit basis vectors [14], and $l = j \pm 1, j$. By expressing the expansion of Eq. (19) in terms of the harmonics (20), one obtains the operators

$$T^l_{jm} = \frac{1}{4\pi i^{j-\epsilon}}\int d\hat{\mathbf{q}}\left[\mathbf{Y}^l_{jm}(\hat{\mathbf{q}})\cdot\mathbf{J}(\mathbf{q}, \omega, P_i)\right]. \quad (21)$$

These operators are irreducible tensors of rank $j$. In accordance with the expressions for the harmonics $\mathbf{Y}^{\rm el,mag}_{jm}$, in terms of the harmonics, Eq. (20) [14], one has

$$\hat{T}^{\rm el}_{jm} = \left(\frac{j+1}{2j+1}\right)^{1/2}\hat{T}^{j-1}_{jm} + \left(\frac{j}{2j+1}\right)^{1/2}\hat{T}^{j+1}_{jm}, \quad (22)$$

$$\hat{T}^{\rm mag}_{jm} = \hat{T}^j_{jm}. \quad (23)$$

Expressions for the components of the multipoles (21) pertaining to the current (11) are listed in the Appendix. The alternative expression for electric multipoles of the current also contains the multipoles,

$$\rho_{jm}(q, \omega) = \frac{1}{4\pi i^j}\int d\hat{\mathbf{q}}Y_{jm}(\hat{\mathbf{q}})\rho(\mathbf{q}, \omega), \quad (24)$$

of the charge density operator.

The dynamical part of the calculation of the response function $R^{\rm ANB}_T$ (7) is performed in the same way as for the laboratory response function in Ref. [4].

## IV. RESULTS AND DISCUSSION

As mentioned in the Introduction we use the AV18 *NN* potential and the UIX 3NF as the nuclear force. The calculation is carried out in the ANB frame for eight momentum transfers $q_{\rm ANB}$: 400, 450, 500, 550, 600, 650, 700, and 750 MeV/$c$. We consider electric and magnetic multipole contributions up to a maximal total angular momentum $J^{\rm max}_f$ of the final state such that a convergent result of $R_T$ is obtained for any $q$ value. For instance, we take $J^{\rm max}_f = 19/2$ and $37/2$ for $q = 400$ and 750 MeV/$c$, respectively. As already pointed out we use the Lorentz integral transform (LIT) formalism [7,8] to take into

[1] In Ref. [1] the spin-orbit contribution to the charge was listed with a misprint; it included $G_M$ instead of $2G_M$. The actual calculation was performed with the correct expression.

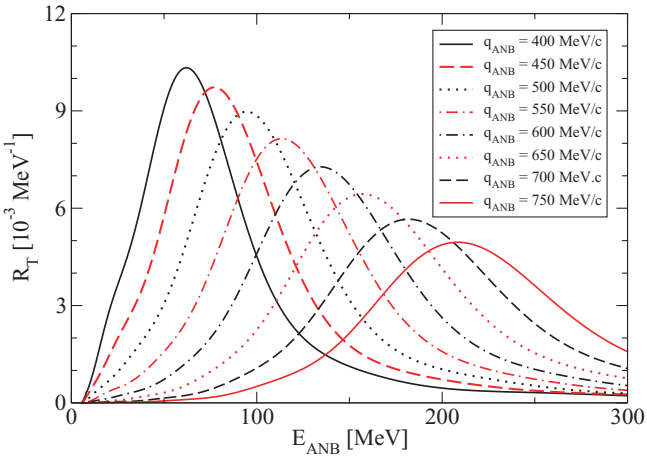


FIG. 1. (Color online) $R_T(q_{\rm ANB}, E_{\rm ANB})$ of $^3$He with relativistic one-body and meson exchange current at various $q$ values (internal excitation energy $E_{\rm ANB} = \omega_{\rm ANB} + q^2_{\rm ANB}/M_T$).

account the final-state interaction. For the LIT parameter $\sigma_I$ we choose two values, namely, $\sigma_{I,1} = 5$ MeV and $\sigma_{I,2} = 50$ MeV. We combine both results in the following way:

$$L_{\rm tot}(\sigma_R, \sigma_I) = L(\sigma_R, \sigma_{I,1}) f(\sigma_R) + \left(\frac{\sigma_{I,2}}{\sigma_{I,1}}\right)^2 L(\sigma_R, \sigma_I)[1 - f(\sigma_R)], \qquad (25)$$

where $L$ denotes the Lorentz transforms of the response, and

$$f(\sigma_R) = \exp[-(\sigma_R/\sigma_0)^6] (\sigma_R \geqslant 0) \quad \text{and} \quad f(\sigma_R) = 1 (\sigma_R \leqslant 0), \qquad (26)$$

with $\sigma_0 = 100$ MeV. This choice has the advantage that one has a relatively large resolution for the $R_T$ behavior at lower energies, while for the high-energy behavior a smaller resolution is completely sufficient. The integral equation that corresponds to the transform $L_{\rm tot}$ was solved to extract $R_T$. The inversion of the LIT [15–17] was done as described in Ref. [4].

In Fig. 1 we show $R_T(q_{\rm ANB}, \omega_{\rm ANB})$ for the previously mentioned eight $q$ values using our full current operator (relativistic one-body + isovector MEC consistent with AV18). One sees that the $q_{\rm ANB}$ dependence of $R_T$ exhibits a very regular and smooth pattern. This allows us to use a spline interpolation to determine $R_T(q_{\rm ANB}, \omega_{\rm ANB})$ for intermediate $q_{\rm ANB}$ values. In this way we are able to obtain results for $R_T(q_{\rm lab}, \omega_{\rm lab})$ via the transformation of Eq.(5) for 500 MeV/$c \leqslant q_{\rm lab} \leqslant$ 700 MeV/$c$.

In the following we investigate three theoretical aspects: (i) comparison of laboratory and ANB frame calculations, (ii) relativistic contributions to the one-body current operator, and (iii) the MEC contribution. We first turn to the comparison of laboratory and ANB frame results. In Fig. 2 we show $R_T(q_{\rm lab}, \omega_{\rm lab})$ evaluated with the nonrelativistic one-body current for laboratory and ANB frame calculations. The ANB results show a sizable shift of the peak position to lower energies, which grows with increasing $q$. In detail one has the following shifts: 8.7, 16.7, and 29.3 MeV at $q = 500$, 600, and 700 MeV/$c$. The size of the shifts is very similar

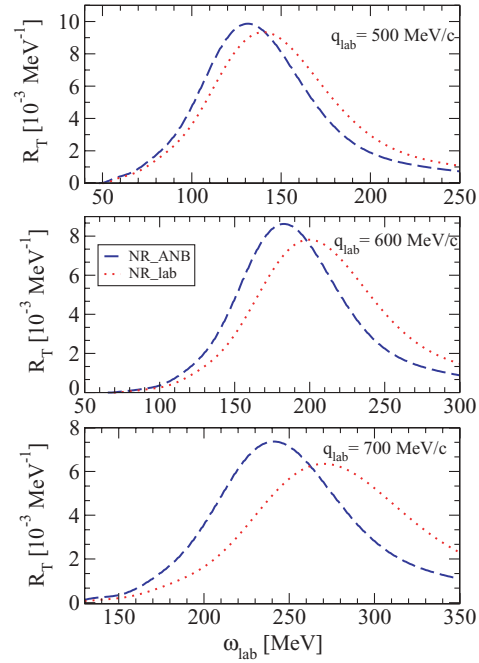


FIG. 2. (Color online) $R_T(q_{\rm lab}, \omega_{\rm lab})$ of $^3$He from ANB (dashed line) and laboratory (dotted line) frame calculations with nonrelativistic one-body current.

to that found for the longitudinal response function $R_L$ in [5] and corresponds to the differences of nonrelativistic and relativistic kinetic energies of a nucleon with momentum $q_{\rm lab}$ (see discussion of peak position in Sec. III). One also finds an increase in the peak heights, namely, by 5.6%, 10.3%, and 16.7%. The relativistic contribution to the one-body current is illustrated in Fig. 3. It leads to a reduction of the peak heights of 6.2%, 8.5%, and 11.3% at $q = 500$, 600, and 700 MeV/$c$, while there are no sizable effects on the peak position. Finally Fig. 4 shows the MEC contributions. As one might expect they are rather small and decrease with increasing $q$. In detail one has increases of 3.2%, 2.7%, and 2.2% for the three considered $q$ values.

Now we turn to a comparison with experimental data (see Fig. 5). For all three momentum transfers considered, one finds an excellent agreement of experimental and theoretical peak positions. For $q = 500$ MeV/$c$ one also has an excellent agreement of the peak height. At $q = 600$ and 700 MeV/$c$ the theoretical peak height overestimates the data by about 5% and 10%, respectively. We would like to mention that a different choice for the nucleon form factor fits should lead to only rather small effects. The reason is that at higher momentum transfer $R_T$ is dominated by the spin current contribution, where the magnetic nucleon form factors enter, which for the various fits are rather similar, in the range 500 MeV/$c \leqslant q \leqslant$ 700 MeV/$c$ (e.g., compare the dipole fits with those in Ref. [18]). In the present work we do not consider any $\Delta$ degrees of freedom. As shown in Ref. [2], up to $q = 500$ MeV/$c$ there are only tiny $\Delta$ effects in the quasielastic region. Also, at higher $q$ one may expect that the quasielastic response is not affected much by $\Delta$ isobar currents (compare to deuteron electrodisintegration results;

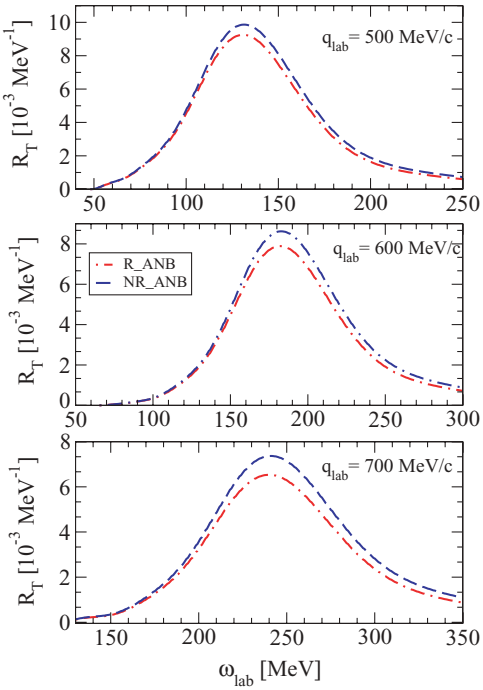


FIG. 3. (Color online) $R_T(q_{\rm lab}, \omega_{\rm lab})$ of $^3$He from ANB frame calculation with relativistic (dash-dotted line) and nonrelativistic (dashed line) one-body current.

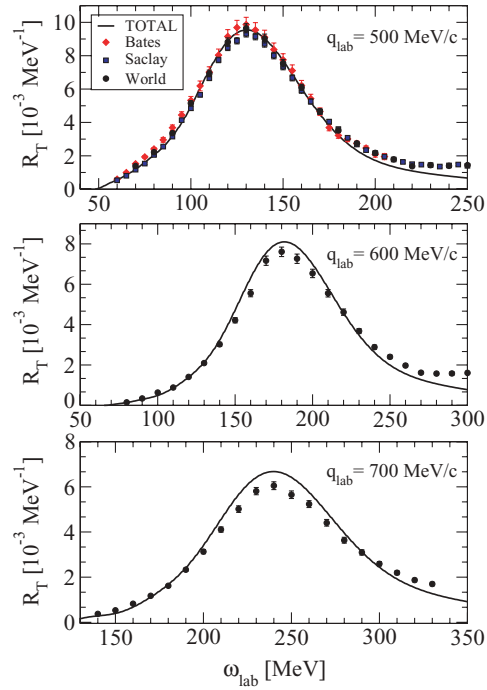


FIG. 5. (Color online) $R_T(q_{\rm lab}, \omega_{\rm lab})$ of $^3$He from ANB frame calculation with relativistic one-body and meson exchange current (solid line) in comparison with experimental results from Ref. [20] (squares), Ref. [21] (diamonds), and Ref. [22] (circles).

see, e.g., Ref. [19]). The increasing difference between theory and experiment with growing momentum transfer suggests that unincluded relativistic effects (wave function boost, dynamical effects) are increasing in importance. Wave function boost

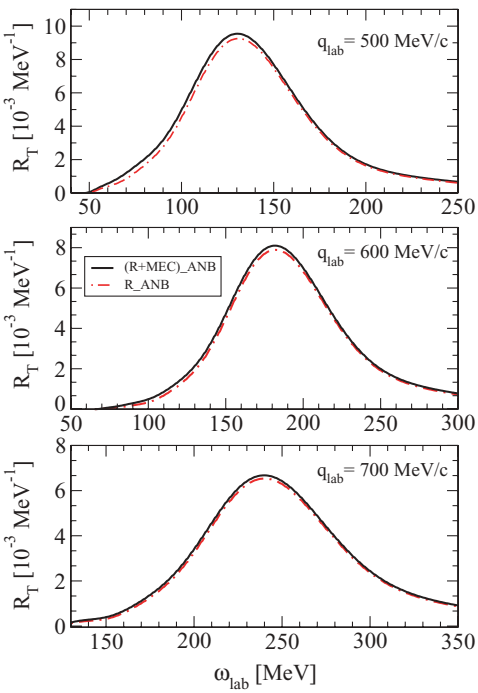


FIG. 4. (Color online) $R_T(q_{\rm lab}, \omega_{\rm lab})$ of $^3$He from ANB frame calculation with relativistic one-body current with (solid line) and without (dash-dotted line) meson exchange current.

effects have already been considered in realistic few-body calculations, namely, in deuteron electrodisintegration [6] and in the $pd$ scattering process [23]. In future we will investigate to see if we can get a better understanding of these effects to improve the comparison with experiment.

For the comparison with the experimental data in Fig. 5, one must consider that pion production is not taken into account in our calculation. The pion production thresholds are at about 180, 200, and 220 MeV at $q = 500$, 600, and 700 MeV/$c$, respectively. For $q = 500$ MeV/$c$ one can see nicely from the figure that the theoretical $R_T$ starts to underestimate the experimental $R_T$ in the pion threshold region. Because the pion production channel is not included in our calculation, this is what one would expect.

To sum up we can say the following. We have calculated the $^3$He transverse response function $R_T(q, \omega)$ with a realistic nuclear force (AV18 two-nucleon and UIX three-nucleon potential) in the quasielastic region at 500 MeV/$c \leqslant q \leqslant$ 700 MeV/$c$ with full inclusion of the final-state interaction. The calculation is carried out in the ANB frame, with subsequent transformation of $R_T$ to the laboratory system. Relativistic effects of the one-body current operator as well as MECs are taken into account. Our calculation shows that the effects owing to the relativistic one-body current reduce the quasielastic peak height, while the MEC contributions are rather unimportant. The use of the ANB frame provides an excellent agreement with experimental peak positions. Concerning the peak heights one finds a good agreement of theoretical and experimental results at $q = 500$ MeV/$c$, while theory overestimates data up to 10% at higher $q$.

## ACKNOWLEDGMENTS

The authors acknowledge the financial support from RFBR Grant No. 07-02-01222-a and RMES Grant No. NS-3004.2008.2 (V.D.E.) and from the National Science and Engineering Research Council of Canada (E.L.T.).


## APPENDIX: MULTIPOLES OF THE ONE-BODY CURRENT AND CHARGE OPERATORS

In the formulas below we use the notation

$$\psi_j = j_j(qr')Y_{jm}(\hat{\mathbf{r}}'), \qquad \Pi_a = \sqrt{2a+1},$$
$$\Pi_{ab} = \sqrt{(2a+1)(2b+1)}.$$

The following quantity $\partial'_\mu$ is defined by the relationship $-i\partial'_\mu = p'_\mu$, and $X_{\gamma\mu} = (\partial' \otimes \partial')_{\gamma\mu}$. Denoting $-i\vec{\partial}'^{(A)} = \mathbf{p}'_A$, where $\mathbf{p}'_A$ is the last particle internal momentum, one has

$$\partial'^{(A)}_\mu = \left[\frac{A-1}{A}\right]^{1/2} \frac{\partial}{\partial \xi_{A-1,\mu}}.$$

Here the derivative is taken with respect to a component of the last Jacobi vector defined as $\vec{\xi}_{A-1} = \sqrt{(A-1)/A}[\mathbf{r}_A - (A-1)^{-1}\sum_{i=1}^{A-1}\mathbf{r}_i]$.

Various operators entering the current, Eq. (11), make the following contributions to the multipoles (21):

$$(4\pi i^{j-1})^{-1}\int d\hat{\mathbf{q}} e^{i\mathbf{q}\mathbf{r}'} i\left(\mathbf{Y}^j_{jm}(\hat{\mathbf{q}})\cdot[\vec{\sigma}\times\hat{\mathbf{q}}]\right) = \left(\frac{j}{2j+1}\right)^{1/2}(\psi_{j+1}\otimes\sigma)_{jm} - \left(\frac{j+1}{2j+1}\right)^{1/2}(\psi_{j-1}\otimes\sigma)_{jm}, \tag{A1}$$

$$(4\pi i^{j})^{-1}\int d\hat{\mathbf{q}} e^{i\mathbf{q}\mathbf{r}'} i\left(\mathbf{Y}^{j+1}_{jm}(\hat{\mathbf{q}})\cdot[\vec{\sigma}\times\hat{\mathbf{q}}]\right) = -\left(\frac{j}{2j+1}\right)^{1/2}(\psi_{j}\otimes\sigma)_{jm}, \tag{A2}$$

$$(4\pi i^{j})^{-1}\int d\hat{\mathbf{q}} e^{i\mathbf{q}\mathbf{r}'} i\left(\mathbf{Y}^{j-1}_{jm}(\hat{\mathbf{q}})\cdot[\vec{\sigma}\times\hat{\mathbf{q}}]\right) = -\left(\frac{j+1}{2j+1}\right)^{1/2}(\psi_{j}\otimes\sigma)_{jm}. \tag{A3}$$

$$(4\pi i^{j-1})^{-1}\int d\hat{\mathbf{q}} e^{i\mathbf{q}\mathbf{r}'}\left(\mathbf{Y}^j_{jm}(\hat{\mathbf{q}})\cdot\mathbf{p}'\right) = (\psi_j\otimes\partial')_{jm}, \tag{A4}$$

$$(4\pi i^{j})^{-1}\int d\hat{\mathbf{q}} e^{i\mathbf{q}\mathbf{r}'}\left(\mathbf{Y}^{j\pm1}_{jm}(\hat{\mathbf{q}})\cdot\mathbf{p}'\right) = \pm(\psi_{j\pm1}\otimes\partial')_{jm}. \tag{A5}$$

$$(4\pi i^{j-1})^{-1}\int d\hat{\mathbf{q}} e^{i\mathbf{q}\mathbf{r}'}\left(\mathbf{Y}^j_{jm}(\hat{\mathbf{q}})\cdot\hat{\mathbf{q}}\right) = 0, \tag{A6}$$

$$(4\pi i^{j})^{-1}\int d\hat{\mathbf{q}} e^{i\mathbf{q}\mathbf{r}'}\left(\mathbf{Y}^{j+1}_{jm}(\hat{\mathbf{q}})\cdot\hat{\mathbf{q}}\right) = -\left(\frac{j+1}{2j+1}\right)^{1/2}\psi_{jm}, \tag{A7}$$

$$(4\pi i^{j})^{-1}\int d\hat{\mathbf{q}} e^{i\mathbf{q}\mathbf{r}'}\left(\mathbf{Y}^{j-1}_{jm}(\hat{\mathbf{q}})\cdot\hat{\mathbf{q}}\right) = \left(\frac{j}{2j+1}\right)^{1/2}\psi_{jm}. \tag{A8}$$

$$(4\pi i^{j-1})^{-1}\int d\hat{\mathbf{q}} e^{i\mathbf{q}\mathbf{r}'}\left(\mathbf{Y}^j_{jm}(\hat{\mathbf{q}})\cdot\mathbf{p}'\right)(\mathbf{p}'\cdot\hat{\mathbf{q}}) = \sqrt{5j}\begin{Bmatrix}1 & 1 & 2\\ j-1 & j & j\end{Bmatrix}(\psi_{j-1}\otimes X_2)_{jm} + \sqrt{5(j+1)}\begin{Bmatrix}1 & 1 & 2\\ j+1 & j & j\end{Bmatrix}(\psi_{j+1}\otimes X_2)_{jm}, \tag{A9}$$

$$(4\pi i^{j})^{-1}\int d\hat{\mathbf{q}} e^{i\mathbf{q}\mathbf{r}'}\left(\mathbf{Y}^{j+1}_{jm}(\hat{\mathbf{q}})\cdot\mathbf{p}'\right)(\mathbf{p}'\cdot\hat{\mathbf{q}}) = -U^{j+2}_j, \tag{A10}$$

$$(4\pi i^{j})^{-1}\int d\hat{\mathbf{q}} e^{i\mathbf{q}\mathbf{r}'}\left(\mathbf{Y}^{j-1}_{jm}(\hat{\mathbf{q}})\cdot\mathbf{p}'\right)(\mathbf{p}'\cdot\hat{\mathbf{q}}) = U^j_j, \tag{A11}$$

$$U^\lambda_j = \sqrt{\lambda-1}\sum_{\gamma=0,2}\Pi_\gamma\begin{Bmatrix}1 & 1 & \gamma\\ \lambda-2 & j & \lambda-1\end{Bmatrix}(\psi_{\lambda-2}\otimes X_\gamma)_{jm} + \sqrt{\lambda}\sum_{\gamma=0,2}\Pi_\gamma\begin{Bmatrix}1 & 1 & \gamma\\ \lambda & j & \lambda-1\end{Bmatrix}(\psi_{\lambda}\otimes X_\gamma)_{jm}. \tag{A12}$$

$$(4\pi i^{j-1})^{-1}\int d\hat{\mathbf{q}} e^{i\mathbf{q}\mathbf{r}'}\left(\mathbf{Y}^j_{jm}(\hat{\mathbf{q}})\cdot\hat{\mathbf{q}}\right)(\mathbf{p}'\cdot\hat{\mathbf{q}}) = 0, \tag{A13}$$

$$(4\pi i^{j})^{-1}\int d\hat{\mathbf{q}} e^{i\mathbf{q}\mathbf{r}'}\left(\mathbf{Y}^{j+1}_{jm}(\hat{\mathbf{q}})\cdot\hat{\mathbf{q}}\right)(\mathbf{p}'\cdot\hat{\mathbf{q}}) = \sqrt{j+1}S, \tag{A14}$$

$$(4\pi i^{j})^{-1}\int d\hat{\mathbf{q}} e^{i\mathbf{q}\mathbf{r}'}\left(\mathbf{Y}^{j-1}_{jm}(\hat{\mathbf{q}})\cdot\hat{\mathbf{q}}\right)(\mathbf{p}'\cdot\hat{\mathbf{q}}) = -\sqrt{j}S, \tag{A15}$$

$$S = (2j+1)^{-1}[\sqrt{j}(\psi_{j-1}\otimes\partial')_{jm} + \sqrt{j+1}(\psi_{j+1}\otimes\partial')_{jm}]. \tag{A16}$$

$$(4\pi i^{j-1})^{-1}\int d\hat{\mathbf{q}} e^{i\mathbf{q}\mathbf{r}'} i\left(\mathbf{Y}^j_{jm}(\hat{\mathbf{q}})\cdot[\vec{\sigma}\times\hat{\mathbf{q}}]\right)(\mathbf{p}'\cdot\hat{\mathbf{q}}) = \left[\frac{(j+1)}{(2j-1)(2j+1)}\right]^{1/2}[\sqrt{j-1}((\psi_{j-2}\otimes\partial')_{j-1}\otimes\sigma)_{jm} + \sqrt{j}((\psi_j\otimes\partial')_{j-1}\otimes\sigma)_{jm}] - \left[\frac{j}{(2j+1)(2j+3)}\right]^{1/2}[\sqrt{j+1}((\psi_j\otimes\partial')_{j+1}\otimes\sigma)_{jm} + \sqrt{j+2}((\psi_{j+2}\otimes\partial')_{j+1}\otimes\sigma)_{jm}]. \tag{A17}$$

$$(4\pi i^{j})^{-1}\int d\hat{\mathbf{q}} e^{i\mathbf{q}\mathbf{r}'} i\left(\mathbf{Y}^{j+1}_{jm}(\hat{\mathbf{q}})\cdot[\vec{\sigma}\times\hat{\mathbf{q}}]\right)(\mathbf{p}'\cdot\hat{\mathbf{q}}) = \sqrt{j}S, \tag{A18}$$

$$(4\pi i^{j})^{-1}\int d\hat{\mathbf{q}} e^{i\mathbf{q}\mathbf{r}'} i\left(\mathbf{Y}^{j-1}_{jm}(\hat{\mathbf{q}})\cdot[\vec{\sigma}\times\hat{\mathbf{q}}]\right)(\mathbf{p}'\cdot\hat{\mathbf{q}}) = \sqrt{j+1}S, \tag{A19}$$

$$S = (2j+1)^{-1}[\sqrt{j}((\psi_{j-1}\otimes\partial')_j\otimes\sigma)_{jm} + \sqrt{j+1}((\psi_{j+1}\otimes\partial')_j\otimes\sigma)_{jm}]. \tag{A20}$$

$$
\begin{aligned}
&(4\pi i^{j-1})^{-1}\int d\hat{\mathbf{q}}e^{i\mathbf{q}\mathbf{r}'}i\left(\mathbf{Y}^{j}_{jm}(\hat{\mathbf{q}})\cdot[\mathbf{p}'\times\hat{\mathbf{q}}]\right)(\vec{\sigma}\cdot\hat{\mathbf{q}})\\
&\quad=\left[\frac{(j-1)(j+1)}{2j+1}\right]^{1/2}\Pi_{j-1}\begin{Bmatrix}1 & j-2 & j-1\\ 1 & j & j-1\end{Bmatrix}((\psi_{j-2}\otimes\partial')_{j-1}\otimes\sigma)_{jm}\\
&\quad-\left[\frac{j(j+1)}{2j+1}\right]^{1/2}\sum_{l=j\pm1,j}(-1)^{l-j}\Pi_l\left[\begin{Bmatrix}1 & j & j-1\\ 1 & j & l\end{Bmatrix}-\begin{Bmatrix}1 & j & j+1\\ 1 & j & l\end{Bmatrix}\right]((\psi_j\otimes\partial')_l\otimes\sigma)_{jm}\\
&\quad-\left[\frac{j(j+2)}{2j+1}\right]^{1/2}\Pi_{j+1}\begin{Bmatrix}1 & j+2 & j+1\\ 1 & j & j+1\end{Bmatrix}((\psi_{j+2}\otimes\partial')_{j+1}\otimes\sigma)_{jm},
\end{aligned}
\tag{A21}
$$

$$
(4\pi i^{j})^{-1}\int d\hat{\mathbf{q}}e^{i\mathbf{q}\mathbf{r}'}i(\mathbf{Y}^{j+1}_{jm}(\hat{\mathbf{q}})\cdot[\mathbf{p}'\times\hat{\mathbf{q}}])(\vec{\sigma}\cdot\hat{\mathbf{q}})=\sqrt{j}S,
\tag{A22}
$$

$$
(4\pi i^{j})^{-1}\int d\hat{\mathbf{q}}e^{i\mathbf{q}\mathbf{r}'}i\left(\mathbf{Y}^{j-1}_{jm}(\hat{\mathbf{q}})\cdot[\mathbf{p}'\times\hat{\mathbf{q}}]\right)(\vec{\sigma}\cdot\hat{\mathbf{q}})=\sqrt{j+1}S,
\tag{A23}
$$

$$
\begin{aligned}
S=&\left(\frac{j}{2j+1}\right)^{1/2}\sum_{l=j-1,j}(-1)^{l-j}\Pi_l\begin{Bmatrix}1 & j-1 & j\\ 1 & j & l\end{Bmatrix}\\
&((\psi_{j-1}\otimes\partial')_l\otimes\sigma)_{jm}+\left(\frac{j+1}{2j+1}\right)^{1/2}\sum_{l=j,j+1}(-1)^{l-j}\Pi_l\\
&\begin{Bmatrix}1 & j+1 & j\\ 1 & j & l\end{Bmatrix}((\psi_{j+1}\otimes\partial')_l\otimes\sigma)_{jm}.
\end{aligned}
\tag{A24}
$$

$$
\begin{aligned}
&(4\pi i^{j-1})^{-1}\int d\hat{\mathbf{q}}e^{i\mathbf{q}\mathbf{r}'}i\left(\mathbf{Y}^{j}_{jm}(\hat{\mathbf{q}})\cdot[\mathbf{p}'\times\hat{\mathbf{q}}]\right)(\vec{\sigma}\cdot\mathbf{p}')\\
&\quad=-\left(\frac{j+1}{2j+1}\right)^{1/2}\sum_{\gamma=0,2}\sum_{l}\Pi_{l\gamma}\begin{Bmatrix}1 & 1 & \gamma\\ l & j-1 & j\end{Bmatrix}\\
&\qquad((\psi_{j-1}\otimes X_\gamma)_l\otimes\sigma)_{jm}+\left(\frac{j}{2j+1}\right)^{1/2}\sum_{\gamma=0,2}\sum_{l}\Pi_{l\gamma}\\
&\qquad\begin{Bmatrix}1 & 1 & \gamma\\ l & j+1 & j\end{Bmatrix}((\psi_{j+1}\otimes X_\gamma)_l\otimes\sigma)_{jm},
\end{aligned}
\tag{A25}
$$

$$
\begin{aligned}
&(4\pi i^{j})^{-1}\int d\hat{\mathbf{q}}e^{i\mathbf{q}\mathbf{r}'}i\left(\mathbf{Y}^{j+1}_{jm}(\hat{\mathbf{q}})\cdot[\mathbf{p}'\times\hat{\mathbf{q}}]\right)(\vec{\sigma}\cdot\mathbf{p}')\\
&\quad=\left(\frac{j}{2j+1}\right)^{1/2}S,\\
&(4\pi i^{j})^{-1}\int d\hat{\mathbf{q}}e^{i\mathbf{q}\mathbf{r}'}i\left(\mathbf{Y}^{j-1}_{jm}(\hat{\mathbf{q}})\cdot[\mathbf{p}'\times\hat{\mathbf{q}}]\right)(\vec{\sigma}\cdot\mathbf{p}')\\
&\quad=\left(\frac{j+1}{2j+1}\right)^{1/2}S,
\end{aligned}
$$

$$
S=\sum_{\gamma=0,2}\sum_{l}\Pi_{l\gamma}\begin{Bmatrix}1 & 1 & \gamma\\ l & j & j\end{Bmatrix}((\psi_j\otimes X_\gamma)_l\otimes\sigma)_{jm}.
\tag{A26}
$$

$$
\begin{aligned}
&(4\pi i^{j-1})^{-1}\int d\hat{\mathbf{q}}e^{i\mathbf{q}\mathbf{r}'}i\left(\mathbf{Y}^{j}_{jm}(\hat{\mathbf{q}})\cdot[\vec{\sigma}\times\mathbf{p}']\right)\\
&\quad=-\sqrt{6}\sum_{l=j\pm1,j}\Pi_l\begin{Bmatrix}1 & 1 & 1\\ j & j & l\end{Bmatrix}((\psi_j\otimes\partial')_l\otimes\sigma)_{jm}.
\end{aligned}
\tag{A27}
$$

$$
\begin{aligned}
&(4\pi i^{j})^{-1}\int d\hat{\mathbf{q}}e^{i\mathbf{q}\mathbf{r}'}i\left(\mathbf{Y}^{j\pm1}_{jm}(\hat{\mathbf{q}})\cdot[\vec{\sigma}\times\mathbf{p}']\right)\\
&\quad=\pm\sqrt{6}\sum_{l}\Pi_l\begin{Bmatrix}1 & 1 & 1\\ j\pm1 & j & l\end{Bmatrix}((\psi_{j\pm1}\otimes\partial')_l\otimes\sigma)_{jm}.
\end{aligned}
\tag{A28}
$$

In deriving these formulas the expressions for $\mathbf{n}\cdot\mathbf{Y}^{l}_{jm}(\mathbf{n})$ in terms of spherical harmonics, and for $\mathbf{n}Y_{jm}(\mathbf{n})$ and $[\mathbf{n}\times\mathbf{Y}^{l}_{jm}(\mathbf{n})]$ in terms of vector spherical harmonics [14], were used. We also used the relationship

$$
\begin{aligned}
(\mathbf{n}\cdot\mathbf{a})(\mathbf{Y}^{l}_{jm}(\mathbf{n})\cdot\mathbf{b})=&\left(\frac{l}{2l+1}\right)^{1/2}((Y_{l-1}(\mathbf{n})\otimes a)_l\otimes b)_{jm}\\
&-\left(\frac{l+1}{2l+1}\right)^{1/2}((Y_{l+1}(\mathbf{n})\otimes a)_l\otimes b)_{jm}.
\end{aligned}
$$

The spin-orbit component of the charge density operator, Eq. (18), in Eq. (24) leads to the multipoles,

$$
\begin{aligned}
&(4\pi i^{j})^{-1}\int d\hat{\mathbf{q}}e^{i\mathbf{q}\mathbf{r}'}Y_{jm}(\hat{\mathbf{q}})i(\vec{\sigma}\cdot[\hat{\mathbf{q}}\times\mathbf{p}'])\\
&\quad=\sqrt{6}\sum_{l}\Pi_l\left[\left(\frac{j}{2j+1}\right)^{1/2}\begin{Bmatrix}1 & 1 & 1\\ j+1 & j & l\end{Bmatrix}\right.\\
&\qquad\left.((\psi_{j+1}\otimes\partial')_l\otimes\sigma)_{jm}\right].
\end{aligned}
\tag{A29}
$$

[1] V. D. Efros, W. Leidemann, G. Orlandini, and E. L. Tomusiak, Phys. Rev. C **69**, 044001 (2004).
[2] A. Deltuva, L. P. Yuan, J. Adam Jr., and P. U. Sauer, Phys. Rev. C **70**, 034004 (2004).
[3] J. Golak, R. Skibinski, H. Witala, W. Glöckle, A. Nogga, and H. Kamada, Phys. Rep. **415**, 89 (2005).
[4] S. Della Monaca, V. D. Efros, A. Khugaev, W. Leidemann, G. Orlandini, E. L. Tomusiak, and L. P. Yuan, Phys. Rev. C **77**, 044007 (2008).
[5] V. D. Efros, W. Leidemann, G. Orlandini, and E. L. Tomusiak, Phys. Rev. C **72**, 011002(R) (2005).
[6] F. Ritz, H. Göller, T. Wilbois, and H. Arenhövel, Phys. Rev. C **55**, 2214 (1997).
[7] V. D. Efros, W. Leidemann, and G. Orlandini, Phys. Lett. **B338**, 130 (1994).
[8] V. D. Efros, W. Leidemann, G. Orlandini, and N. Barnea, J. Phys. G **34**, R459 (2007).
[9] R. Machleidt. Adv. Nucl. Phys. **19**, 189 (1989).
[10] R. B. Wiringa, V. G. J. Stoks, and R. Schiavilla, Phys. Rev. C **51**, 38 (1995).
[11] B. S. Pudliner, V. R. Pandharipande, J. Carlson, S. C. Pieper, and R. B. Wiringa, Phys. Rev. C **56**, 1720 (1997).
[12] W. Leidemann, V. D. Efros, G. Orlandini, and E. L. Tomusiak, Few-Body Syst. (in press); arXiv:0906.0663.
[13] H. Arenhövel and M. Schwamb, Eur. Phys. J. A **12**, 207 (2001).
[14] D. A. Varshalovich, A. N. Moskalev, and V. K. Khersonskii, *Quantum Theory of Angular Momentum* (Singapore, World Scientific, 1988).
[15] V. D. Efros, W. Leidemann, and G. Orlandini, Few-Body Syst. **26**, 251 (1999).
[16] D. Andreasi, W. Leidemann, Ch. Reiss, and M. Schwamb, Eur. Phys. J. A **24**, 361 (2005).
[17] N. Barnea, V. D. Efros, W. Leidemann, and G. Orlandini, arXiv:0906.5421.
[18] P. Mergell, U.-G. Meissner, and D. Drechsel, Nucl. Phys. **A596**, 367 (1996).
[19] H. Arenhövel, W. Leidemann, and E. L. Tomusiak, Eur. Phys. J. A **23**, 147 (2005).
[20] C. Marchand *et al.*, Phys. Lett. **B153**, 29 (1985).
[21] K. Dow *et al.*, Phys. Rev. Lett. **61**, 1706 (1988).
[22] J. Carlson, J. Jourdan, R. Schiavilla, and I. Sick, Phys. Rev. C **65**, 024002 (2002).
[23] H. Witala, J. Golak, W. Glöckle, and H. Kamada, Phys. Rev. C **71**, 054001 (2005).